Science Bulletin 70 (2025) 842–846

Contents lists available at ScienceDirect

Science Bulletin

journal homepage: www.elsevier.com/locate/scib

Short Communication

NAT10 primes a post-transcriptional repertoire essential for the maintenance of spermatogonial homeostasis

Xiaoli Zhu [a,1], Caoling Xu [a,1], Xue Jiang [a], Jiaqi Zou [a], Wenqing Li [a], Xuemei Xing [a], Xiaoxiao Gao [a], Jiao Lei [b], Fei Meng [b], Xin Wang [d], Yuzhang Zhu [a], Yu Cheng [e], Muhammad Azhar [a], Wenjie Han [f], Ge Lin [b,c], Yunfang Zhang [d,*], Ge Shan [f,*], Shen Zhang [b,c,*], Jianqiang Bao [a,f,*]

[a] Center for Reproduction and Genetics, The First Affiliated Hospital of USTC, Division of Life Sciences and Medicine, University of Science and Technology of China, Hefei 230001, China
[b] Clinical Research Center for Reproduction and Genetics in Hunan Province, Reproductive and Genetic Hospital of CITIC-XIANGYA, Changsha 410000, China
[c] NHC Key Laboratory of Human Stem Cell and Reproductive Engineering, School of Basic Medical Sciences, Central South University, Changsha 410075, China
[d] Clinical and Translational Research Center of Shanghai First Maternity and Infant Hospital, Shanghai Key Laboratory of Signaling and Disease Research, Frontier Science Center for Stem Cell Research, School of Life Sciences and Technology, Tongji University, Shanghai 200092, China
[e] School of Information Science and Technology, University of Science and Technology of China (USTC), Hefei 230001, China
[f] Center for Advanced Interdisciplinary Science and Biomedicine of IHM, Hefei National Laboratory for Physical Sciences at Microscale, Biomedical Sciences and Health Laboratory of Anhui Province, University of Science and Technology of China (USTC), Hefei 230001, China

ARTICLE INFO

Article history:
Received 24 August 2024
Received in revised form 24 October 2024
Accepted 24 December 2024
Available online 15 January 2025

Male fertility is built on the proper proliferation and differentiation of germline cells within the seminiferous epithelium in the testis, which continuously produces millions of sperm per day in mammals [1]. RNA modifications are emerging as crucial epitranscriptomic regulators, with diverse roles in a wide range of biological processes [2,3]. N4-acetylcytidine (ac^4C) is highly conserved across prokaryotes and eukaryotes, and is catalyzed by the solely known enzyme "writer," N-acetyltransferase 10 (NAT10) [4,5]. NAT10 is closely involved in meiotic progression in both male spermatocytes and female oocytes in mice [6,7]. However, the functional importance and the molecular mechanisms by which NAT10-mediated ac^4C modification coordinates the complex, premeiotic process remain poorly understood.

To investigate the role of Nat10 in spermatogonia, we examined testicular 10× single-cell mRNA datasets (E-MTAB-6946) alongside our immunofluorescence staining and western blotting results. The analyses revealed that NAT10 is a nucleolar protein predominantly expressed in spermatogonia in both mouse and human testes (Figs. S1 and S2 online). To further explore NAT10's function in spermatogonial development, we employed two germline-specific *Nat10* knockout mouse models: the *Nat10*-ScKO model, created by crossing *Stra8-Cre* mice with $Nat10^{lox/lox}$ mice (Fig. S3 online), and the *Nat10*-DcKO model, a *Ddx4*-promoter-driven, tamoxifen-inducible *Nat10* knockout model generated by intercrossing our in-house customized Ddx4-CreERT2 mice ($C57BL/6JDdx4^{tm1(5\times HA\text{-}P2A\text{-}EGFP\text{-}T2A\text{-}CreERT2)Bao}$) with $Nat10^{lox/lox}$ mice (mouse experiments were approved by the Ethics Committee of University of Science and Technology of China (USTC) (ethical approval No. USTCACUC25120124040)) (Fig. S5a and b online). *Nat10* knockout in both mouse models resulted in infertility with significantly reduced testicular sizes (Figs. S4a, b and S5c, d online). Histological analysis revealed a prominent loss of germ cells upon *Nat10* KO (Figs. S4c, d and S5e online). Immunofluorescence staining and western blotting revealed comparable numbers of PLZF-positive spermatogonia in postnatal day 7 (P7) testes; however, by P12, most germ cells were depleted in *Nat10*-ScKO testes, (Fig. S4e–j online). In comparison, the numbers for both undifferentiated and differentiated spermatogonia were significantly reduced in *Nat10*-DcKO testes at P7 (Fig. S5f–n online). These findings suggest that NAT10 is essential for spermatogonial proliferation and differentiation.

Then we injected $Nat10^{lox/lox}$;$Ddx4^{GFP\text{-}CreERT2}$ mice between P8–P10 to delete the *Nat10* gene in pre-leptotene spermatocytes (Fig. S6a–c online). The testes from WT and *Nat10*-DcKO mice appeared morphologically similar, with seemingly normal meiotic

* Corresponding authors.
E-mail addresses: zhangyunfang@tongji.edu.cn (Y. Zhang), shange@ustc.edu.cn (G. Shan), szhang231@126.com (S. Zhang), jqbao@ustc.edu.cn (J. Bao).
[1] These authors contributed equally.

https://doi.org/10.1016/j.scib.2025.01.021

DSB repair, although some zygotene spermatocytes were dysregulated in *Nat10*-DcKO mice (Figs. S6d, e and S7a–h online). In adult mice, by 32 d post-tamoxifen (dpt), *Nat10*-DcKO testes exhibited a "Sertoli cell only" phenotype, which was not observed before 18 dpt (Figs. S6f–h and S7i, j online). These data indicate that NAT10 is essential for maintaining steady-state homeostasis of spermatogonia in adult testes.

We next explored the transcriptomic changes in *Nat10-null* spermatogonia. Spermatogonial cells were purified via fluorescence-activated cell sorting (FACS) using EGFP reporter in Ddx4-CreERT2 model [7,8]. The results revealed similar numbers of up- and down-regulated genes, with Gene Ontology (GO) analysis indicating that down-regulated genes were primarily associated with the cell cycle and cell division (Fig. S8a–d online). Additionally, key genes involved in spermatogonial proliferation and differentiation, including *Ccna2*, *Ccnb2*, *Sox3*, *Dmrt1*, *Stra8*, and *lin28a*, were significantly downregulated (Fig. S8e–g online). We further verified these findings by measuring mRNA levels of cell-cycle regulators in tamoxifen-inducible *Nat10* knockout mouse embryonic fibroblast (MEF) cell lines [7], demonstrating significant downregulation of cell-cycle genes such as *Ccnb2*, *Ccna2*, *Ccne1*, *Ccnd1*, *Cdc20*, and *Cdca3* (Fig. S8h online). Strikingly, attempts to produce a *Nat10* homozygous knockout cell line in F9, a testicular teratoma-derived cell line, failed, suggesting that *Nat10-null* mutation causes cell lethality (Fig. S9 online). Collectively, these data suggest that NAT10 regulates a common set of cell-cycle genes crucial for cell viability.

Since NAT10 is the only known "writer" of the ac^{4}C, we further carried out liquid chromatography/mass spectrometry (LC-MS/MS) analysis to analyze the RNA modifications. Our findings revealed that ac^{4}C levels were significantly lower in *Nat10*-depleted testes (Fig. S10a–d online). NAT10 requires a cofactor for ac^{4}C deposition in 18S rRNAs and tRNAs in mammalian cells [5,9], but global snoRNA (SNORD13) knockout models have shown that NAT10/SNORD13-mediated ac^{4}C modification of rRNA does not affect cell survival or proliferation [10], suggesting ac^{4}C mark on rRNA is dispensable for cellular development. We next assessed whether NAT10/THUMPD1-deposited ac^{4}C modification in tRNAs functions in mammalian cells. We generated two stable *Thumpd1* knockout F9 cell lines (Fig. S11 online). Only ac^{4}C levels in tRNAs were significantly lower in *Thumpd1*-null F9 cells (Fig. S10e–g online), supporting the previous notion that NAT10 partners with THUMPD1 to deposit ac^{4}C in tRNAs [5]. Notably, however, the protein translation, cell proliferation or apoptosis was indistinguishable between *Thumpd1-null* and WT F9 cells (Fig. S10h–j online). These data rule out the possibility that NAT10/THUMPD1-deposited ac^{4}C in tRNAs is responsible for cell lethality in both germline and somatic cells.

Given these findings, we next reasoned that NAT10-deposited ac^{4}C in mRNAs might account for the deleterious effects. To this end, we deciphered the ac^{4}C-modified mRNA landscape using an in-house optimized ac^{4}C-RIP-seq protocol in pubertal mouse testes (Fig. 1a). Consistent with prior studies [4], most ac^{4}C-enriched peaks were located across the 5′UTR and coding sequence region (CDS) of mRNA transcripts (Fig. 1b and Fig. S12a–d online). GO enrichment analysis suggested that ac^{4}C-modified mRNAs were primarily associated with cell cycles and cell differentiation (Fig. 1c), while transcripts without ac^{4}C showed no significant difference between up- and down-regulated mRNAs (Fig. 1d, e and Fig. S12e, f online). These data suggest that NAT10 stabilizes mRNA transcripts by depositing the ac^{4}C mark. The ac^{4}C-positive mRNAs that were only down-regulated upon *Nat10* loss comprised a cohort of representative genes in relation to cell proliferation/differentiation and the cell cycle (Fig. 1f and Fig. S12g, h online). Both visual inspection and ac^{4}C-RIP-PCR/qPCR assays confirmed that *Dmrt1*, *Six5*, *Sox3*, and *Ccna2* are ac^{4}C-modified by NAT10 (Fig. 1g–h). An *in vitro* mRNA decay assay revealed that the *Dmrt1* and *Sox3* mRNA stability was significantly reduced in *Nat10*-deficient testes (Fig. S12i online). Together, this evidence suggests that mRNA ac^{4}C modification accounts for spermatogonial defects upon *Nat10* KO.

Prior studies imply that ac^{4}C modification is associated with enhanced mRNA translation [4,7], we employed an in-house optimized Ribo-seq assay [7,11] (Fig. 1i), which demonstrated high quality and reproducibility. However, following *Nat10* deletion, the majority of RPF transcripts were downregulated (Fig. S13a–f online), suggesting global translational repression upon *Nat10* loss. Combined with RNA-seq data, the downregulated genes exhibited declined RPF occupancy and were primarily enriched in pathways related to the cell cycle and germline development (Fig. 1j, k). Notably, the number of genes exhibiting up- or down-regulation at the mRNA levels was similar for transcripts with elevated RPFs. Further analysis revealed that more of the downregulated genes also showed decreased translation levels (Fig. S13g, h online). Moreover, we observed a greater number of ac^{4}C-positive mRNAs with decreased RPF intensity in *Nat10*-deficient testes compared with WT testes (423 vs. 262) (Fig. 1l). These mRNAs were involved in cell cycle, multicellular organism development, and cell differentiation (Fig. 1m). We also validated the expression of representative downregulated genes from Ribo-seq and mRNA-seq (Fig. S13i–m online). These findings underscore the critical role of NAT10 in enhancing the translation of ac^{4}C-modified mRNA substrates, particularly those involved in cell cycle and germline development.

To further explore these changes at proteome level, we conducted label-free quantitative MS (Fig. 2a), which identified dysregulated proteins in *Nat10*-deficient testes (up: down, 326:296) (Fig. 2b). GO enrichment analysis revealed that these proteins were closely associated with cell cycle, cell division, proliferation, and germline development (Fig. 2c). We overlapped the dysregulated proteins with the gene transcripts detected by Ribo-seq and found 43% of the downregulated proteins exhibited reduced RPF occupancy (Fig. 2d). Furthermore, among the genes with downregulated RPFs, mRNA transcripts, and ac^{4}C-positive transcripts, a total of 280 transcripts were commonly enriched in cell cycle and multicellular development (Fig. 2e, f). We intersected the downregulated proteins with the shared 280 transcripts and identified six ac^{4}C-modified genes, including *Dmrt1* and *Ccna2*, that are subject to attenuated gene expression regulation (Fig. 2g and Fig. S14a online). These results were further validated by qPCR and immunoblotting (Fig. 2h–j). Collectively, these integrative analyses unambiguously showed that, at least in part, both DMRT1 and CCNA2 are *bona fide* substrates for NAT10-catalyzed ac^{4}C modification *in vivo*, responsible for defective spermatogonial homeostasis.

To interrogate which cofactors interplay with NAT10 to deposit ac^{4}C modification, we optimized an in-house, sensitive "on-beads" protein digestion protocol designed for immunoprecipitation mass spectrometry (IP-MS) using testicular spermatogonia and F9 cells. We introduced a Flag-SBP-HA(FSH) tag in-frame at the N-terminus of the NAT10 protein, and confirmed its expression (Fig. 2k and Fig. S15 online). After normalization, we identified 254 and 333 unique NAT10-interacting proteins in F9 cells and P7 testes, respectively (Fig. 2l). GO enrichment classified these proteins as primarily related to cell cycle, mRNA processing, and translation (Fig. S14b online). Of interest, motif conservation analysis and functional screening established PRRC2B as the principal NAT10-interacting protein by recognizing the conserved motif "CuuCcUCcU" (Fig. 2m and Table S3 online) [12,13]. PRRC2B associates with NAT10 in an RNA-dependent manner, which was corroborated through co-immunoprecipitation, as well as by the colocalization of the two proteins in the nuclei via immunofluorescence staining (Fig. 2n, o). Further, the knockdown assay using two siRNAs against *Prrc2b* confirmed that PRRC2B is critical for the expression of genes targeted by NAT10-mediated ac^{4}C deposition,

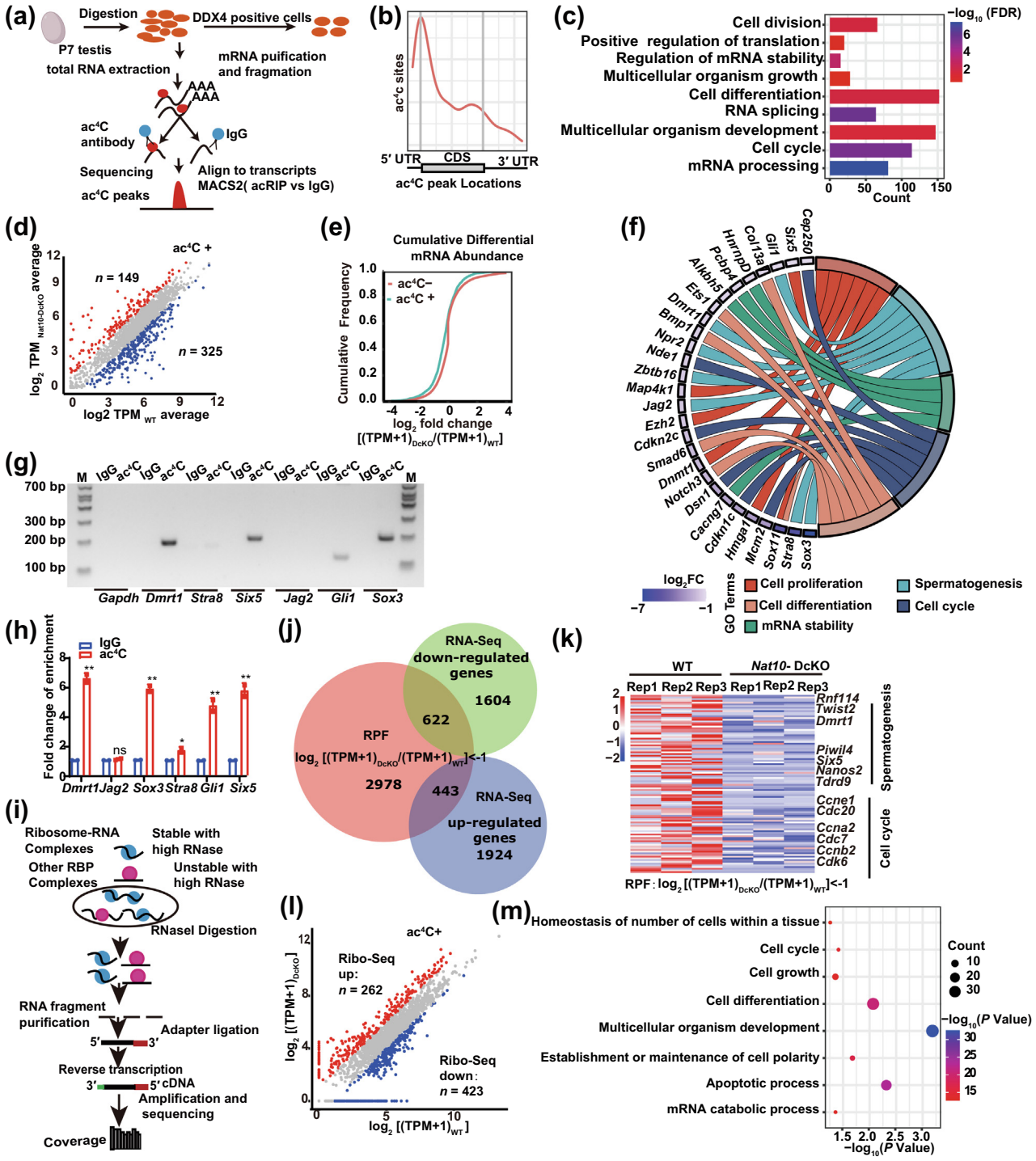

Fig. 1. NAT10 mediates the post-transcriptional expression regulation of a cohort of mRNA substrates in an ac^{4}C-dependent manner. (a) Schematic overview for ac^{4}C-RIP-Seq workflow. (b) Distribution of ac^{4}C-enriched peaks across the full length of mRNAs. (c) Functional terms enriched for the ac^{4}C target genes. (d) Scatter plot showing the numbers of up- and down-regulated gene transcripts among the ac^{4}C target genes. (e) Cumulative distribution function (CDF) plot depicting differential expression of ac^{4}C-negative (ac^{4}C$^-$) or ac^{4}C-positive (ac^{4}C$^+$) transcripts in the NAT10 versus IgG group. ($P < 0.0001$, Mann-Whitney test). (f) Functional annotation of representative overlapping genes among down-regulated genes and ac^4 C target genes. (g, h) Validation of ac^{4}C peaks for representative genes using acRIP-PCR and acRIP-qPCR. ***$P < 0.001$; n.s., not significant; Student's *t*-test. (i) Schematic for the Ribo-Seq workflow and library preparation. (j) Venn diagram comparing the overlapping gene transcripts between the DEGs and the down-regulated transcripts by Ribo-Seq in *Nat10*-DcKO testis at P7. (k) Integrated analysis of commonly down-regulated genes by RNA-seq and Ribo-Seq. (l) Scatter plot comparing transcript RPFs among ac^{4}C-positive target genes. RPF values were calculated via average TPM+1 between *Nat10*-DcKO and WT testes at P7. Gene transcripts with RPFs dys-regulated ≥2-fold are in red and blue, respectively. (m) Functional annotation of representative overlapping genes between those down-regulated in Ribo-Seq and ac^{4}C target genes.

as well as for cell proliferation (Fig. 2p, q and Fig. S14c–f online). Together, these data identify PRRC2B as an intimate *in vivo* cofactor of NAT10, potentially facilitating the deposition of the ac^{4}C mark on NAT10 mRNA substrates.

In this study, we exploited our highly efficient, tamoxifen-inducible *Nat10* KO mouse models, and revealed a prominent role of NAT10 in priming a coordinated post-transcriptional repertoire in testicular spermatogonia during both first-wave spermatogene-

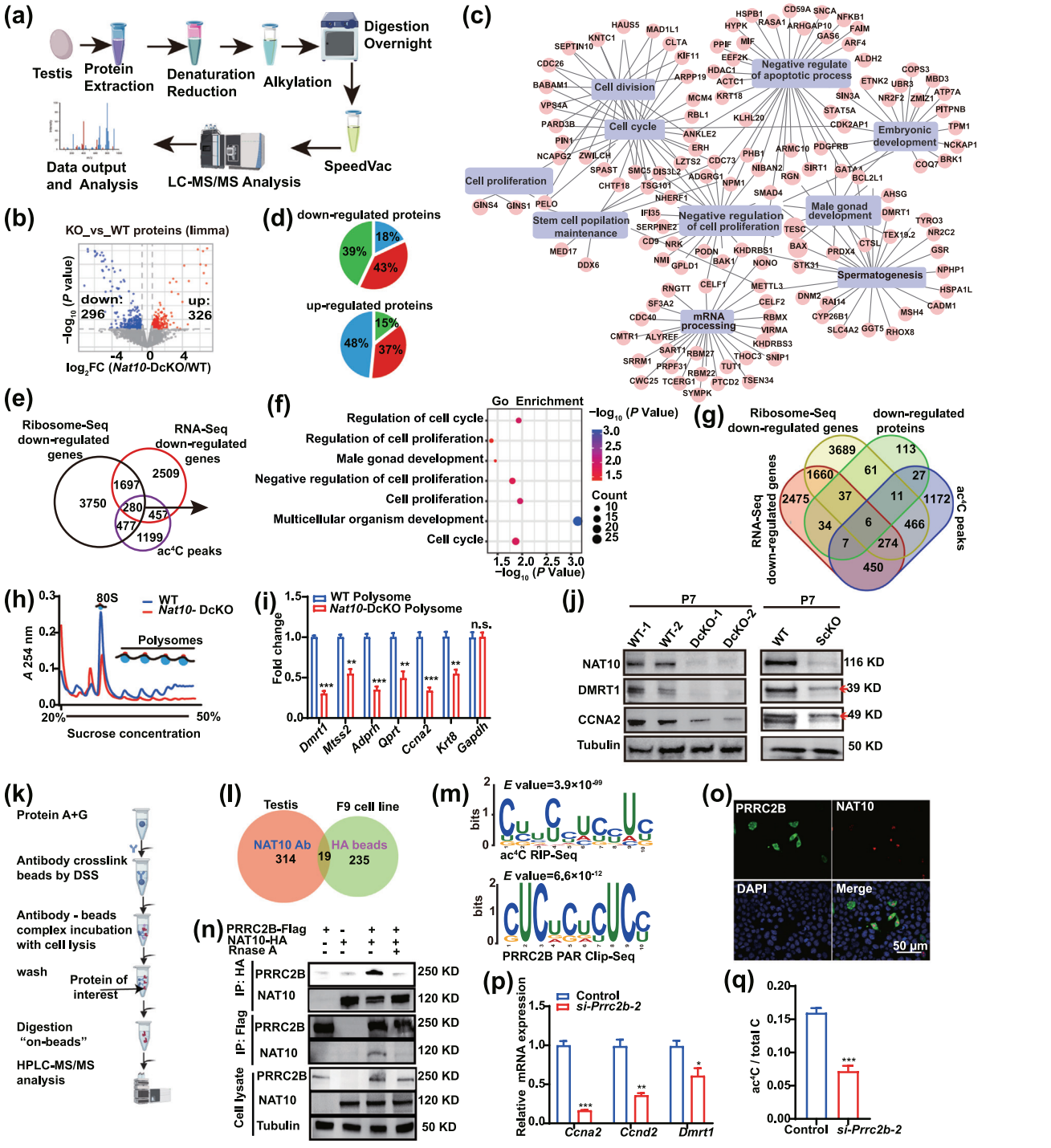

Fig. 2. Multi-omic analyses identified a NAT10 cofactor, PRRC2B, in post-transcriptionally regulating DMRT1 and CCNA2 substrates. (a) Workflow for identification of differentially expressed proteins (DEPs) upon *Nat10* KO. (b) Volcano plot showing significant DEPs in the *Nat10*-DcKO testis at P7. (c) Major GO terms associated with DEPs in (b). (d) Pie charts showing translatome-wide distribution of DEPs (RPF: green, up-regulated; red, down-regulated; blue, not significant). (e) Integrated analysis of the gene transcripts by overlapping among ac^{4}C peaks, the down-regulated mRNAs and RPFs in the testes of *Nat10*-DcKO mice. (f) GO terms enriched in the significantly DEGs in (e). (g) Venn diagram showing NAT10-responsive ac^{4}C target genes by combinatorial analysis of the mRNA-Seq, Ribo-Seq, and proteomic data. (h) Global analysis of the translational activity in P7 mouse testes using polysome profiling. (i) qPCR assay showing the relatively declined mRNA levels of the six overlapping genes from polysome profiling in *Nat10*-DcKO testes. $^{**}P < 0.01$, $^{***}P < 0.001$, n.s., not significant; Student's *t*-test. (j) Validation of protein expression levels for key genes involved in spermatogonial development upon *Nat10* KO ($n = 3$ for biological replicates). (k) Workflow for identification of NAT10-interacting proteins. (l) Venn diagram of NAT10-interacting proteins identified in the testes and F9 cell line. (m) The top hit of enriched consensus motifs deduced from ac^{4}C-RIP-Seq data, compared with published PRRC2B PAR Clip-Seq data, by MEME [12]. (n)Reciprocal co-immunoprecipitation validating the interaction between NAT10 and PRRC2B, with or without RNase A treatment. (o) Immunofluorescence co-staining of NAT10 (red) and PRRC2B (green) in the C18-4 cell line. The nuclei were stained with DAPI (blue). Scale bar, 50 μm. (p) Detection of ac^{4}C-positive target gene expression of Nat10 following *Prrc2b* knockdown by RT-qPCR. (q) Quantification of ac^{4}C modification levels upon *Prrc2b* knockdown in C18-4 cell line. Data are presented as the mean ± SEM; $^{*}P < 0.05$, $^{**}P < 0.01$, $^{***}P < 0.001$.

sis and adult steady-state spermatogenesis. Through integrative analysis of RNA-seq, ac^{4}C-RIP-seq, Ribo-seq, and proteomic data, we identified DMRT1 and CCNA2 as downstream ac^{4}C-modified substrates of NAT10. Remarkably, knockout mouse models for either *Dmrt1* or *Ccna2* phenocopied the spermatogonial defects observed in *Nat10* knockout mice [14,15]. Additionally, we identified PRRC2B as a key partner that assists NAT10 *in vivo*. These findings not only enhance our understanding of the mechanisms underlying spermatogonial development at the epitranscriptomic level, but also provide valuable insights for future functional studies on NAT10 substrates and cofactors in other milieux.

Conflict of interest

The authors declare that they have no conflict of interest.

Acknowledgments

This work was supported by the National Key Research and Development Program of China (2019YFA0802600, 2022YFC2702600), Research Funds of Center for Advanced Interdisciplinary Science and Biomedicine of IHM" (QYPY20230032), the National Natural Science Foundation of China (31970793, 32170856 and 32300711), the Anhui Provincial Natural Science Foundation grant (2408085J016), the Reproductive and Genetic Hospital of CITIC-XIANGYA (YNXM-202211), the Hunan Provincial Grant for Innovative Province Construction (2019SK4012) and the Hundred Youth Talents Program of Hunan Province.

Author contributions

JianQiang Bao, XiaoLi Zhu, Shen Zhang, Ge Shan and YunFang Zhang conceived, designed, and supervised the work. JianQiang Bao and XiaoLi Zhu wrote the manuscript. XiaoLi Zhu, Xue Jiang and JiaQi Zou performed mouse crossing, chromosome spreads analysis, immunofluorescent staining. CaoLing Xu and XiaoXiao Gao analyzed the omics data. WenQing Li did plasmids construction. XueMei Xing did HE staining of mouse testis with the help of YuZhang Zhu, Yu Cheng, Muhammad Azhar. Jiao Lei and Fei Meng performed the proteomics analysis. Xin Wang did the experiment on RNA modification detection. Wen-Jie Han and Ge Lin modified the manuscript.

Data availability

All the raw data and processed files have been deposited in the Sequence Read Archive (SRA) (https://www.ncbi.nlm.nih.gov/sra) with the accession numbers: PRJNA1082542 and PRJNA1082548. All MS data were deposited in the ProteomeXchange Consortium (https://proteomecentral.proteomexchange.org) via the PRIDE partner repository with the identifier PXD050145.

Appendix A. Supplementary material

Supplementary data to this article can be found online at https://doi.org/10.1016/j.scib.2025.01.021.

References

[1] Hess RA, Renato de Franca L. Spermatogenesis and cycle of the seminiferous epithelium. Adv Exp Med Biol 2008;636:1–15.
[2] Roundtree IA, Evans ME, Pan T, et al. Dynamic RNA modifications in gene expression regulation. Cell 2017;169:1187–200.
[3] Gilbert WV, Nachtergaele S. Mrna regulation by RNA modifications. Annu Rev Biochem 2023;92:175–98.
[4] Arango D, Sturgill D, Alhusaini N, et al. Acetylation of cytidine in mRNA promotes translation efficiency. Cell 2018;175:e1824.
[5] Sharma S, Langhendries JL, Watzinger P, et al. Yeast Kre33 and human NAT10 are conserved 18S rRNA cytosine acetyltransferases that modify tRNAs assisted by the adaptor Tan1/THUMPD1. Nucleic Acids Res 2015;43:2242–58.
[6] Chen L, Wang WJ, Liu Q, et al. NAT10-mediated N4-acetylcytidine modification is required for meiosis entry and progression in male germ cells. Nucleic Acids Res 2022;50:10896–913.
[7] Jiang X, Cheng Y, Zhu Y, et al. Maternal NAT10 orchestrates oocyte meiotic cell-cycle progression and maturation in mice. Nat Commun 2023;14:3729.
[8] Azhar M, Xu C, Jiang X, et al. The arginine methyltransferase Prmt1 coordinates the germline arginine methylome essential for spermatogonial homeostasis and male fertility. Nucleic Acids Res 2023;51:10428–50.
[9] Sharma S, Yang J, van Nues R, et al. Specialized box C/D snoRNPs act as antisense guides to target RNA base acetylation. PLoS Genet 2017;13:e1006804.
[10] Bortolin-Cavaille ML, Quillien A, Thalalla Gamage S, et al. Probing small ribosomal subunit RNA helix 45 acetylation across eukaryotic evolution. Nucleic Acids Res 2022;50:6284–99.
[11] Li Q, Yang H, Stroup EK, et al. Low-input RNase footprinting for simultaneous quantification of cytosolic and mitochondrial translation. Genome Res 2022;32:545–57.
[12] Bailey TL, Johnson J, Grant CE, et al. The meme suite. Nucleic Acids Res 2015;43:W39–49.
[13] Jiang F, Hedaya OM, Khor E, et al. RNA binding protein PRRC2B mediates translation of specific mRNAs and regulates cell cycle progression. Nucleic Acids Res 2023;51:5831–46.
[14] Raymond CS, Murphy MW, O'Sullivan MG, et al. *Dmrt1*, a gene related to worm and fly sexual regulators, is required for mammalian testis differentiation. Genes Dev 2000;14:2587–95.
[15] Ma F, Wang X, Chung SSW, et al. Cyclin A2 is essential for mouse gonocyte maturation. Cell Cycle 2020;19:1654–64.